

How to approach continuum physics in the lattice Weinberg-Salam model

M. A. Zubkov*

ITEP, Bolshaja Cherjemushkinskaya 25, Moscow, 117259, Russia

(Received 7 September 2010; published 16 November 2010)

We investigate the lattice Weinberg-Salam model without fermions numerically for the realistic choice of coupling constants correspondent to the value of the Weinberg angle $\theta_W \sim 30^\circ$, and bare fine structure constant around $\alpha \sim \frac{1}{150}$. We consider the values of the scalar self-coupling corresponding to Higgs mass $M_H \sim 100, 150, 270$ GeV. It has been found that nonperturbative effects become important while approaching continuum physics within the lattice model. When the ultraviolet cutoff $\Lambda = \frac{\pi}{a}$ (where a is the lattice spacing) is increased and achieves the value around 1 TeV, one encounters the fluctuational region (on the phase diagram of the lattice model), where the fluctuations of the scalar field become strong. The classical Nambu monopole can be considered as an embryo of the unphysical symmetric phase within the physical phase. In the fluctuational region quantum Nambu monopoles are dense, and therefore, the use of the perturbation expansion around the trivial vacuum in this region is limited. Further increase of the cutoff is accompanied by a transition to the region of the phase diagram, where the scalar field is not condensed (this happens at the value of Λ around 1.4 TeV for the considered lattice sizes). Within this region further increase of the cutoff is possible, although we do not observe this in detail due to the strong fluctuations of the gauge boson correlator. Both above mentioned regions look unphysical. Therefore we come to the conclusion that the maximal value of the cutoff admitted within lattice electroweak theory cannot exceed the value of the order of 1 TeV.

DOI: 10.1103/PhysRevD.82.093010

PACS numbers: 12.15.-y, 11.15.Ha, 12.10.Dm

I. INTRODUCTION

It is well-known [1] that the finite temperature perturbation expansion breaks down at the temperatures above the electroweak transition/crossover already for Higgs masses above about 60 GeV. Therefore the present lower bound on the Higgs mass requires the use of nonperturbative techniques while investigating electroweak physics at high temperature.

Nambu monopoles are not described by means of a perturbation expansion around the trivial vacuum background. Therefore, nonperturbative methods should be used in order to investigate their physics. However, their mass is estimated at the TeV scale. That is why at zero temperature and at the energies much less than 1 TeV their effect on physical observables is negligible. However, when energy of the processes approaches 1 TeV we expect these objects to influence the dynamics. Recently the indications in favor of this point of view were indeed found [2–4].

In this paper we consider lattice realization of zero temperature electroweak theory (without fermions). The phase diagram of the correspondent lattice model contains the physical Higgs phase, where the scalar field is condensed and gauge bosons Z and W acquire their masses. This physical phase is bounded by the phase-transition surface. Crossing this surface one leaves the Higgs phase and enters the phase of the lattice theory, where the scalar field is not condensed.

In the lattice theory the ultraviolet cutoff is finite and is equal to the momentum $\Lambda = \frac{\pi}{a}$ (see, for example, [5]), where a is the lattice spacing. The physical scale can be fixed, for example, using the value of the Z -boson mass $M_Z^{\text{phys}} \sim 90$ GeV. Therefore the lattice spacing is evaluated to be $a \sim [90 \text{ GeV}]^{-1} M_Z$, where M_Z is the Z -boson mass in lattice units. Within the physical phase of the theory the lines of constant physics (LCP) are defined that correspond to constant renormalized physical couplings (the fine structure constant α , the Weinberg angle θ_W , and Higgs mass to Z -boson mass ratio $\eta = M_H/M_Z$). The points on LCP are parametrized by the lattice spacing. Our observation is that the LCP corresponding to realistic values of α , θ_W , and η crosses the transition between the two “phases” at a certain value $a = a_c$ and for $a < a_c$ the scalar field is not condensed. We denote the corresponding value of the cutoff $\Lambda_c = \frac{\pi}{a_c}$. Our estimate for the considered values of the Higgs mass $M_H \sim 100, 160, 270$ GeV is $\Lambda_c = 1.4 \pm 0.2$ TeV (for the considered lattice sizes). We do not observe the dependence of Λ_c on the lattice size. That is why the value Λ_c might appear as the maximal possible value of the cutoff allowed in the conventional electroweak theory.

It is important to compare this result with the limitations on the ultraviolet cutoff, which come from the perturbation theory. From the point of view of perturbation theory the energy scale 1 TeV appears in the hierarchy problem [6]. Namely, the mass parameter μ^2 for the scalar field receives a quadratically divergent contribution in one loop. Therefore, the initial mass parameter ($\mu^2 = -\lambda_c v^2$, where v is the vacuum average of the scalar field)

*zubkov@itep.ru

should be set to infinity in such a way that the renormalized mass μ_R^2 remains negative and finite. This is the content of the so-called fine-tuning. It is commonly believed that this fine-tuning is not natural [6] and, therefore, one should set up the finite ultraviolet cutoff Λ . From the requirement that the one-loop contribution to μ^2 is less than $10|\mu_R^2|$, one derives that $\Lambda \sim 1$ TeV. However, strictly speaking, the possibility that the mentioned fine-tuning takes place is not excluded.

In the perturbation theory there is also a more solid limitation on the ultraviolet cutoff. It appears as a consequence of the triviality problem, which is related to Landau pole in the scalar field self-coupling λ and in the fine structure constant α . The Landau pole in the fine structure constant is related to the fermion loops and, therefore, has no direct connection with our lattice result (we neglect dynamical fermions in our consideration). Because of the Landau pole the renormalized λ is zero, and the only way to keep it equal to its measured value is to impose the limitation on the cutoff. That is why the electroweak theory is usually thought of as a finite cutoff theory. For small Higgs masses (less than about 350 GeV) the correspondent energy scale Λ_c^0 calculated within the perturbation theory is much larger than 1 TeV. In particular, for $M_H \sim 300$ GeV we have $\Lambda_c^0 \sim 1000$ TeV. It is worth mentioning that for $\lambda \rightarrow \infty$ the perturbation expansion in λ cannot be used. In this case the Higgs mass approaches its absolute upper bound [7], and both triviality and hierarchy scales approach each other.

From the previous research we know that the phase diagram in the β - γ plane of the lattice $SU(2)$ gauge-Higgs for any fixed λ resembles the phase diagram for the lattice Weinberg-Salam model. The only difference is that in the $SU(2)$ gauge-Higgs model the confinement-deconfinement phase transition corresponding to the $U(1)$ constituents of the model is absent. The direct measurement of the renormalized coupling β_R shows [8–21] that the line of constant renormalized coupling constant (with the value close to the experimental one) intersects the phase-transition line. Also we know from the direct measurements of M_W in the $SU(2)$ gauge-Higgs model that the ultraviolet cutoff is increased when one is moving along this line from the physical Higgs phase to the symmetric phase.

On the tree level the gauge boson mass in lattice units vanishes on the transition surface at small enough λ . This means that the tree level estimate predicts the appearance of an infinite ultraviolet cutoff at the transition point for small λ . At infinite λ the tree level estimate gives nonzero values of lattice masses at the transition point. Our numerical investigation of the $SU(2) \otimes U(1)$ model (at $\lambda = 0.0025, 0.009, 0.001$) and previous calculations in the $SU(2)$ gauge-Higgs model (both at finite λ and at $\lambda = \infty$) showed that for the considered lattice sizes renormalized masses do not vanish and the transition is of either the first

order or a crossover. (Actually, the situation, when the cutoff tends to infinity at the position of the transition point, means that there is a second order phase transition.) The dependence on the lattice sizes for the $SU(2)$ gauge-Higgs model was investigated, for example, in [17]. Namely, for $\beta = 8$, $\lambda \sim 0.0016$, where $M_H \sim M_W$, the correlation lengths were evaluated at the transition points. For different lattice sizes (from $12^3 \times 28$ to $18^3 \times 36$) no change in correlation length was observed [17].

In Table 1 of [2] the data on the ultraviolet cutoff achieved in selected lattice studies of the $SU(2)$ gauge-Higgs model are presented. Everywhere β is around $\beta \sim 8$ and the renormalized fine structure constant is around $\alpha \sim 1/110$. This table shows that the maximal value of the cutoff $\Lambda = \frac{\pi}{a}$ ever achieved in these studies is around 1.4 TeV.

Thus the predictions on the value of Λ_c given by our lattice study and on the value Λ_c^0 given by the perturbation theory contradict with each other. We suggested a possible explanation of this contradiction in [4]. Namely, it was demonstrated that in the vicinity of the transition there exists the fluctuational region. Within this region the application of the perturbation theory is limited. This situation is similar to that of some phenomenological models that describe condensed matter systems [22], where there exists the vicinity of the finite temperature phase transition that is also called the fluctuational region. In this region the fluctuations of the order parameter become strong. The contribution of these fluctuations to certain physical observables becomes larger than the tree level estimate. Thus the perturbation theory in these models fails down within the fluctuational region.

We find that there exists the vicinity of the phase transition between the Higgs phase and the symmetric phase in the Weinberg-Salam model, where the fluctuations of the scalar field become strong and the perturbation expansion around the trivial vacuum cannot be applied. According to the numerical results the continuum theory is to be approached within the vicinity of the phase transition; i.e., the cutoff is increased along the line of constant physics when one approaches the point of the transition. That is why the conventional prediction of the value of the cutoff admitted in the standard model based on the perturbation theory may be incorrect.

In the present paper we proceed to further investigate [4] the model at the value of the scalar self-coupling $\lambda = 0.009$ (which corresponds to the Higgs boson mass around 270 GeV in the vicinity of the phase transition), bare Weinberg angle $\theta_W = 30^\circ$, and bare fine structure constant around $1/150$. The results presented now correspond to essentially larger lattices than that used in [4]. Namely, in [4] the main results correspond to lattices $8^3 \times 16$; some results were checked on the lattice $12^3 \times 16$; two points were checked on the lattice 16^4 . Now our main results are

obtained on the lattice 16^4 , while the results at the transition point were checked on the lattice $20^3 \times 24$.

In addition we investigate the model at the value of the scalar self-coupling $\lambda = 0.0025$, bare Weinberg angle $\theta_W = 30^\circ$, and bare fine structure constant around $\alpha_0 \sim 1/150$. These values of couplings correspond to the Higgs boson mass around 150 GeV in the vicinity of the phase transition. The results are obtained using lattices $8^3 \times 16$, $12^3 \times 16$, and 16^4 . We also present results for $\lambda = 0.001$, $\theta_W = 30^\circ$, $\alpha_0 \sim 1/150$. These values of couplings correspond to the Higgs boson mass around 100 GeV. The results are obtained using lattices $8^3 \times 16$, $12^3 \times 16$.

It is worth mentioning that far from the transition point the renormalized fine structure constant slowly approaches the tree level estimate. Contrary to the maximal value of the cutoff the renormalized fine structure constant depends on the lattice size. And for the larger lattice the value of α_R is closer to the tree level estimate than for the smaller one. For example, for $\beta = 12$, $\gamma \sim 1$, $\lambda = 0.001$ (far from the transition point) on the lattice $8^3 \times 16$, the value of α_R is around $1/130$, while on the lattice $12^3 \times 16$ it is around $1/140$. Within the fluctuational region the deviation from tree level estimate becomes essentially strong. For example, for $\lambda = 0.009$, $\gamma = 0.274$ (near the transition point) the renormalized value of α_R calculated on the lattice $8^3 \times 16$ is around $1/99$, while on the lattice $20^3 \times 24$ its value is around $1/106$. As it is seen from our numerical results and as it will be explained in the conclusions, we guess the mentioned finite volume effects present in the value of renormalized α do not affect the main observables we considered like the value of Λ_c and the Nambu monopole density.

We calculate the constraint effective potential $V(|\Phi|)$ for the Higgs field Φ . In the physical Higgs phase this potential has a minimum at a certain nonzero value ϕ_m of $|\Phi|$. This shows that the spontaneous breakdown of the electroweak symmetry takes place as it should. However, there exists the vicinity of the phase transition, where the fluctuations of the Higgs field are of the order of ϕ_m while the height of the “potential barrier” [23] $H = V(0) - V(\phi_m)$ is of the order of $V(\phi_m + \delta\phi) - V(\phi_m)$, where $\delta\phi$ is the fluctuation of $|\Phi|$. We expect that in this region the perturbation expansion around trivial vacuum $\Phi = (\phi_m, 0)^T$ cannot be applied. This region of the phase diagram is called the fluctuational region (FR).

The nature of the fluctuational region is illustrated by the behavior of quantum Nambu monopoles [24,25]. We show that their lattice density increases when the phase-transition point is approached. Within the FR these objects are so dense that it is not possible at all to speak of them as of single monopoles [26]. Namely, within this region the average distance between the Nambu monopoles is of the order of their size. Such complicated configurations obviously have nothing to do with the conventional vacuum used in the continuum perturbation theory.

II. THE LATTICE MODEL UNDER INVESTIGATION

The lattice Weinberg-Salam Model without fermions contains gauge field $\mathcal{U} = (U, \theta)$ [where $U \in SU(2)$, $e^{i\theta} \in U(1)$ are realized as link variables], and the scalar doublet Φ_α ($\alpha = 1, 2$) defined on sites.

The action is taken in the form

$$S = \beta \sum_{\text{plaquettes}} \left(\left(1 - \frac{1}{2} \text{Tr} U_p \right) + \frac{1}{\text{tg}^2 \theta_W} (1 - \cos \theta_p) \right) + \gamma \sum_{xy} \text{Re}(\Phi^+ U_{xy} e^{i\theta_{xy}} \Phi) + \sum_x (|\Phi_x|^2 + \lambda(|\Phi_x|^2 - 1)^2), \quad (1)$$

where the plaquette variables are defined as $U_p = U_{xy} U_{yz} U_{zw}^* U_{xw}^*$, and $\theta_p = \theta_{xy} + \theta_{yz} - \theta_{zw} - \theta_{xw}$ for the plaquette composed of the vertices x, y, z, w . Here λ is the scalar self-coupling, and $\gamma = 2\kappa$, where κ corresponds to the constant used in the investigations of the $SU(2)$ gauge-Higgs model. θ_W is the Weinberg angle.

Bare fine structure constant α is expressed through β and θ_W as $\alpha = \frac{\text{tg}^2 \theta_W}{\pi \beta (1 + \text{tg}^2 \theta_W)}$. In order to demonstrate this we consider the naïve continuum limit of (1). We set

$$U_{x,\mu} = e^{iA_\mu(x)a}, \quad e^{i\theta_{x,\mu}} = e^{iB_\mu(x)a}. \quad (2)$$

Here a is the lattice spacing. The field $B_\mu = \frac{\tilde{B}_\mu}{2}$, where \tilde{B}_μ , is the conventional $U(1)$ field, while A_μ is the conventional $SU(2)$ field. In continuum limit (1) must become

$$S_g = \int d^4x \left\{ \frac{1}{2g_2^2} \text{Tr} \left[2 \times \sum_{i>j} G_{ij}^2 \right] + \frac{1}{4g_1^2} \left[2 \times \sum_{i>j} \tilde{F}_{ij}^2 \right] \right\}. \quad (3)$$

Here $\tilde{F}_{ij} = \partial_i \tilde{B}_j - \partial_j \tilde{B}_i = 2(\partial_i B_j - \partial_j B_i) = 2F_{ij}$, $G_{ij} = \partial_i A_j - \partial_j A_i - i[A_i, A_j]$. We also have the following correspondence between the plaquette variables and the field strengths:

$$\text{Tr} U_{x,\mu\nu} = \text{Tr} \left[1 - \frac{1}{2} G_{\mu\nu}^2 a^4 \right], \quad \cos N \theta_{x,\mu\nu} = \left[1 - \frac{N^2}{2} F_{\mu\nu}^2 a^4 \right]. \quad (4)$$

Now in order to clarify the correspondence between constants $g_{1,2}$ and β we must substitute the expressions for the field strengths to (1) and compare it to (3). We have

$$\frac{1}{g_1^2} = \frac{1}{4 \text{tg}^2 \theta_W} \times \beta, \quad \frac{1}{g_2^2} = \beta/4. \quad (5)$$

Thus

$$\begin{aligned} \text{tg } \theta_W &= \frac{g_1}{g_2}, \\ \alpha &= \frac{e^2}{4\pi} = \frac{[\frac{1}{g_1^2} + \frac{1}{g_2^2}]^{-1}}{4\pi} = \frac{\text{tg}^2 \theta_W}{\pi\beta(1 + \text{tg}^2 \theta_W)}. \end{aligned} \quad (6)$$

We consider the region of the phase diagram with $\beta \sim 12$ and $\theta_W \sim \pi/6$. Therefore, bare couplings are $\sin^2 \theta_W \sim 0.25$; $\alpha \sim \frac{1}{150}$. These values are to be compared with the experimental ones $\sin^2 \theta_W(100 \text{ GeV}) \sim 0.23$, $\alpha(100 \text{ GeV}) \sim \frac{1}{128}$.

The simulations were performed on lattices of sizes $8^3 \times 16$, $12^3 \times 16$. For $\lambda = 0.0025$, 0.009 we investigate the system on the lattice 16^4 . The transition point at $\lambda = 0.009$ was checked using the larger lattice ($20^3 \times 24$). In order to simulate the system we used the Metropolis algorithm. The acceptance rate is kept around 0.5 via the automatic self-tuning of the suggested distribution of the fields. At each step of the suggestion the random value is added to the old value of the scalar field while the old value of the gauge field is multiplied by a random $SU(2) \otimes U(1)$ matrix. We use the Gaussian distribution for both the random value added to the scalar field and the parameters of the random matrix multiplied by the lattice gauge field. We use two independent parameters for these distributions: one for the gauge fields and another for the scalar field. The program code has been tested for the case of a frozen scalar field. And the results of the papers [3] are reproduced. We also have tested our code for the $U(1)$ field frozen and repeat the results of [27]. Far from the transition point the autocorrelation time for the gauge fields is estimated as about $N_{\text{auto}}^g \sim 500$ Metropolis steps. In the vicinity of the transition point the autocorrelation time is several times larger and is about $N_{\text{auto}}^g \sim 1500$ Metropolis steps. (The correlation between the values of the gauge field is less than 3% for the configurations separated by N_{auto}^g Metropolis steps. Each metropolis step consists of renewing the fields over all the lattice.) The autocorrelation time for the scalar field is essentially smaller than for the gauge fields and is of the order of $N_{\text{auto}}^\phi \sim 20$. The estimated time for preparing the equilibrium starting from the cold start far from the phase transition within the Higgs phase is about 18 000 Metropolis steps for the considered values of couplings. At the same time near the phase transition and within the symmetric phase the estimated time for preparing the equilibrium is up to 3 times larger.

III. THE TREE LEVEL ESTIMATES OF LATTICE QUANTITIES

At finite λ the line of constant renormalized α is not a line of constant physics, because the mass of the Higgs boson depends on the position on this line. Thus, in order to investigate the line of constant physics one should vary λ

together with γ to keep the ratio of lattice masses M_H/M_W constant.

In order to obtain the tree level estimates let us rewrite the lattice action in an appropriate way. Namely, we define the scalar field $\tilde{\Phi} = \sqrt{\frac{\gamma}{2}}\Phi$. We have

$$\begin{aligned} S &= \beta \sum_{\text{plaquettes}} \left(\left(1 - \frac{1}{2} \text{Tr} U_p \right) + \frac{1}{\text{tg}^2 \theta_W} (1 - \cos \theta_p) \right) \\ &+ \sum_{xy} |\tilde{\Phi}_x - U_{xy} e^{i\theta_{xy}} \tilde{\Phi}_y|^2 \\ &+ \sum_x (\mu^2 |\tilde{\Phi}_x|^2 + \tilde{\lambda} |\tilde{\Phi}_x|^4) + \omega, \end{aligned} \quad (7)$$

where $\mu^2 = -2(4 + (2\lambda - 1)/\gamma)$, $\tilde{\lambda} = 4\frac{\lambda}{\gamma^2}$, and $\omega = \lambda V$. Here $V = L^4$ is the lattice volume, and L is the lattice size.

For negative μ^2 we fix unitary gauge $\tilde{\Phi}_2 = 0$, $\text{Im} \tilde{\Phi}_1 = 0$, and introduce the vacuum value of $\tilde{\Phi}$: $v = \frac{|\mu|}{\sqrt{2\tilde{\lambda}}}$. We also introduce the scalar field σ instead of $\tilde{\Phi}$: $\tilde{\Phi}_1 = v + \sigma$. We denote $V_{xy} = (U_{xy}^{11} e^{i\theta_{xy}} - 1)$, and obtain

$$\begin{aligned} S &= \beta \sum_{\text{plaquettes}} \left(\left(1 - \frac{1}{2} \text{Tr} U_p \right) + \frac{1}{\text{tg}^2 \theta_W} (1 - \cos \theta_p) \right) \\ &+ \sum_{xy} ((\sigma_x - \sigma_y)^2 + |V_{xy}|^2 v^2) + \sum_x 2|\mu|^2 \sigma_x^2 \\ &+ \sum_{xy} ((\sigma_y^2 + 2v\sigma_y)|V_{xy}|^2 \\ &- 2(\sigma_x - \sigma_y) \text{Re} V_{xy}(\sigma_y + v)) \\ &+ \sum_x \tilde{\lambda} \sigma_x^2 (\sigma_x^2 + 4v\sigma_x) + \tilde{\omega}, \end{aligned} \quad (8)$$

where $\tilde{\omega} = \omega - \tilde{\lambda} v^4 V$.

Now we easily derive the tree level estimates:

$$\begin{aligned} M_H &= \sqrt{2}|\mu| = 2\sqrt{4 + (2\lambda - 1)/\gamma}; \\ M_W &= \sqrt{2} \frac{v}{\sqrt{\beta}} = \sqrt{\frac{\gamma(4\gamma + 2\lambda - 1)}{2\lambda\beta}}; \\ M_W &= \cos \theta_W M_Z \quad M_H/M_W = \sqrt{8\lambda\beta/\gamma^2}; \\ \Lambda &= \pi \sqrt{\frac{2\lambda\beta}{\gamma(4\gamma + 2\lambda - 1)}} [80 \text{ GeV}]. \end{aligned} \quad (9)$$

The fine structure constant is given by $\alpha = \frac{\text{tg}^2 \theta_W}{\pi\beta(1 + \text{tg}^2 \theta_W)}$ and does not depend on λ and γ . From (9) we learn that at the tree level LCP on the phase diagram corresponds to fixed $\beta = \frac{\text{tg}^2 \theta_W}{\pi\alpha(1 + \text{tg}^2 \theta_W)} \sim 10$ and $\eta = M_H/M_W$, and is given by the equation $\lambda(\gamma) = \frac{\eta^2}{8\beta} \gamma^2$.

The important case is $\lambda = \infty$, where the tree level estimates give

$$M_H = \infty; \quad M_W = \sqrt{\frac{\gamma}{\beta}},$$

$$M_Z = \sqrt{\frac{\gamma}{\beta}} \cos^{-1} \theta_W; \quad \Lambda = \pi \sqrt{\frac{\beta}{\gamma}} [80 \text{ GeV}]. \quad (10)$$

In the $SU(2)$ gauge-Higgs model for the small values of $\lambda \ll 0.1$, the tree level estimate for M_H/M_W gives values that differ from the renormalized ratio by about 20% [18]. The tree level estimate for the ultraviolet cutoff is about 1 TeV at $\lambda = \infty$, $\gamma = 1$, $\beta = 15$, which is not far from the numerical result given in [3]. In the $SU(2)$ gauge-Higgs model at $\lambda = \infty$ the critical $\gamma_c = 0.63$ for $\beta = 8$ [21]. At this point the tree level estimate gives $\Lambda = 0.9 \text{ TeV}$ while the direct measurements give $\Lambda \in [0.8; 1.5] \text{ TeV}$ for values of $\gamma \in [0.64; 0.95]$ [21]. The investigations of the $SU(2)$ gauge-Higgs model showed that a consideration of finite λ does not change much the estimate for the gauge boson mass. However, at finite λ and values of γ close to the phase-transition point, the tree level formula does not work at all.

The tree level estimate for the critical γ is $\gamma_c = (1 - 2\lambda)/4\gamma$. At small λ this formula gives values that are close to the ones obtained by the numerical simulations [19–21]. In particular, $\gamma_c \rightarrow 0.25$ ($\kappa_c \rightarrow 0.125$) at $\lambda \ll 1$. However, this formula clearly does not work for $\lambda > 1/2$. From [19–21, 28] we know that the critical coupling in the $SU(2)$ gauge-Higgs model is about 2–4 times smaller for $\lambda = 0$ than for $\lambda = \infty$.

Tree level estimate predicts that there is the second order phase transition. This means that according to the tree level estimate the value of the cutoff at the transition point is infinite. Our numerical simulations, however, show that the cutoff remains finite and the transition is, most likely, a crossover at the considered values of θ_W , λ , and β .

IV. NAMBU MONOPOLES

In this section we remind the reader of what is called the Nambu monopole [24]. First let us define the continuum electroweak fields as they appear in the Weinberg-Salam model. The continuum scalar doublet is denoted as Φ . The Z -boson field Z^μ and electromagnetic field A_{EM}^μ are defined as

$$Z^\mu = -\frac{1}{\sqrt{\Phi^\dagger \Phi}} \Phi^\dagger A^\mu \Phi - B^\mu, \quad (11)$$

$$A_{\text{EM}}^\mu = 2B^\mu + 2\sin^2 \theta_W Z^\mu,$$

where A^μ and B^μ are the corresponding $SU(2)$ and $U(1)$ gauge fields of the standard model.

After fixing the unitary gauge $\Phi_2 = \text{const}$, $\Phi_1 = 0$ we have

$$Z^\mu = \frac{g_z}{2} \left[\frac{\tilde{A}_3^\mu}{g_2} \cos \theta_W - \frac{\tilde{B}^\mu}{g_1} \sin \theta_W \right] = \frac{1}{2} \tilde{Z}^\mu, \quad (12)$$

$$A_{\text{EM}}^\mu = e \left[\frac{\tilde{A}_3^\mu}{g_2} \sin \theta_W + \frac{\tilde{B}^\mu}{g_1} \cos \theta_W \right] = \tilde{A}^\mu,$$

where $\frac{\tilde{A}_3}{g_2} = \frac{1}{g_2} \text{Tr} A \sigma^3$, $\frac{\tilde{B}}{g_1} = 2B/g_1$, $\frac{\tilde{Z}}{g_z}$, $\frac{\tilde{A}}{e}$ are conventional standard model fields, and $g_z = \sqrt{g_1^2 + g_2^2}$.

Nambu monopoles are defined as the endpoints of the Z string [24]. The Z string is the classical field configuration that represents the object, which is characterized by the magnetic flux extracted from the Z -boson field. Namely, for a small contour C winding around the Z string one should have

$$\int_C Z^\mu dx^\mu \sim 2\pi; \quad \int_C A_{\text{EM}}^\mu dx^\mu \sim 0;$$

$$\int_C B^\mu dx^\mu \sim 2\pi \sin^2 \theta_W. \quad (13)$$

The string terminates at the position of the Nambu monopole. The hypercharge flux is supposed to be conserved at that point. Therefore, a Nambu monopole carries electromagnetic flux $4\pi \sin^2 \theta_W$. The size of Nambu monopoles was estimated [24] to be of the order of the inverse Higgs mass, while its mass should be of the order of a few TeV. According to [24] Nambu monopoles may appear only in the form of a bound state of a monopole-antimonopole pair.

In lattice theory the following variables are considered as creating the Z boson:

$$Z_{xy} = Z_x^\mu = -\sin[\text{Arg}(\Phi_x^\dagger U_{xy} e^{i\theta_{xy}} \Phi_y)] \quad (14)$$

and

$$Z'_{xy} = Z_x^\mu = -[\text{Arg}(\Phi_x^\dagger U_{xy} e^{i\theta_{xy}} \Phi_y)]. \quad (15)$$

The classical solution corresponding to a Z string should be formed around the 2-dimensional topological defect which is represented by the integer-valued field defined on the dual lattice $\Sigma = \frac{1}{2\pi} ([dZ']_{\text{mod } 2\pi} - dZ')$. [Here we used the notations of differential forms on the lattice. For a definition of those notations see, for example, [29]. Lattice field Z' is defined in Eq. (15).] Therefore, Σ can be treated as the world sheet of a quantum Z string [25]. Then, the worldlines of quantum Nambu monopoles appear as the boundary of the Z -string world sheet: $j_Z = \delta \Sigma$.

For historical reasons in lattice simulations we fix unitary gauge $\Phi_2 = 0$, $\Phi_1 \in \mathcal{R}$, $\Phi_1 \geq 0$ (instead of the usual $\Phi_1 = 0$, $\Phi_2 \in \mathcal{R}$), and the lattice electroweak theory becomes a lattice $U(1)$ gauge theory with the $U(1)$ gauge field

$$A_{xy} = A_x^\mu = [Z' + 2\theta_{xy}] \text{ mod } 2\pi. \quad (16)$$

(The usual lattice electromagnetic field is related to A as $A_{EM} = A - Z' + 2\sin^2\theta_W Z'$.) One may try to extract monopole trajectories directly from A . The monopole current is given by

$$j_A = \frac{1}{2\pi} * d([dA] \bmod 2\pi). \quad (17)$$

Both j_Z and j_A carry magnetic charges. That is why it is important to find the correspondence between them.

In continuum notations we have

$$A^\mu = Z^\mu + 2B^\mu, \quad (18)$$

where B is the hypercharge field. Its strength is divergenceless. As a result in continuum theory the net Z flux emanating from the center of the monopole is equal to the net A flux. (Both A and Z are undefined inside the monopole.) This means that in the continuum limit the position of the Nambu monopole must coincide with the position of the antimonopole extracted from the field A . Therefore, one can consider Eq. (17) as another definition of a quantum Nambu monopole [3]. Actually, in our numerical simulations we use the definition of Eq. (17).

V. PHASE DIAGRAM

In our lattice study we fix bare $\theta_W = \pi/6$. Then in the three-dimensional (β, γ, λ) phase diagram the transition surfaces are two-dimensional. The lines of constant physics on the tree level are the lines $(\frac{\lambda}{\gamma^2} = \frac{1}{8\beta} \times (M_H^2/M_W^2) = \text{const}; \beta = \frac{1}{4\pi\alpha} = \text{const})$. We suppose that in the vicinity of the transition the deviation of the lines of constant physics from the tree level estimate may be significant. However, qualitatively their behavior is the same. Namely, the cutoff is increased along the line of constant physics when γ is decreased and the maximal value of the cutoff is achieved at the transition point. Nambu monopole density in lattice units is also increased when the ultraviolet cutoff is increased.

At $\beta = 12$ (corresponds to bare $\alpha \sim 1/150$) the phase diagram is represented in Fig. 1. This diagram is obtained, mainly, using the lattice $8^3 \times 16$. Some regions ($\lambda = 0.009, 0.0025, 0.001$), however, were checked using larger lattices. According to our data there is no dependence of the diagram on the lattice size. The physical Higgs phase is situated right to the transition line. The position of the transition $\gamma_c(\lambda)$ is localized here at the point where the susceptibility extracted from the Higgs field creation operator achieves its maximum. We use the susceptibility

$$\chi = \langle H^2 \rangle - \langle H \rangle^2 \quad (19)$$

extracted from $H = \sum_y Z_{xy}^2$ (see, for example, Fig. 2). We observe no difference between the values of the susceptibility calculated using the lattices of different sizes. This indicates that the transition at γ_c is a crossover. Indeed we find that gauge boson masses do not vanish in a certain

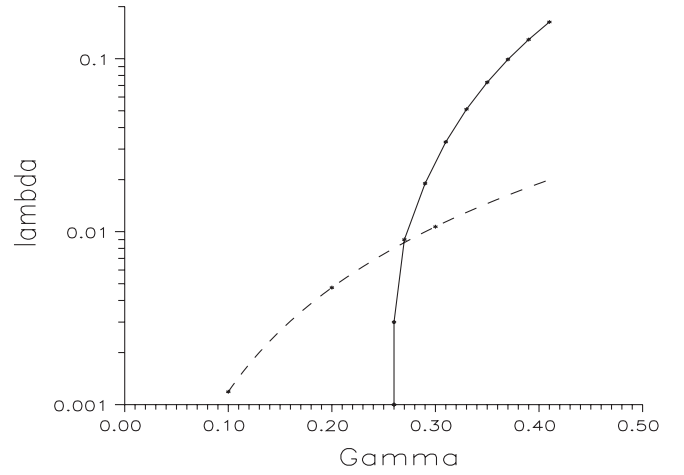


FIG. 1. The phase diagram of the model in the (γ, λ) plane at $\beta = 12$. The dashed line is the tree level estimate for the line of constant physics correspondent to bare $M_H^0 = 270$ GeV. The continuous line is the line of phase transition between the physical Higgs phase and the unphysical symmetric phase (statistical errors for the values of γ at each λ on this line are about 0.005).

vicinity of γ_c even within the symmetric phase. In the next section we shall see that within the statistical errors γ_c coincides with the value of γ , where the scalar field condensate disappears. Actually, there also exist two other crucial points: $\gamma_{c0}(\lambda) < \gamma_c(\lambda) < \gamma_{c2}(\lambda)$ (say, at $\lambda = 0.001$ we have $\gamma_{c0} = 0.252 \pm 0.001$, $\gamma_c = 0.256 \pm 0.001$, $\gamma_{c2} = 0.258 \pm 0.001$; see the next sections for the details). γ_{c2} denotes the boundary of the fluctuational region. At γ_{c0} the extrapolation of the dependence of lattice Z -boson mass $M_Z(\gamma)$ on γ indicates that $M_Z(\gamma_{c0})$ may vanish. In the symmetric phase the perturbation theory predicts vanishing of the gauge boson masses. Therefore, supposition that M_Z vanishes at a certain point is very natural. The perturbation theory also predicts that the mass parameter present in the effective action for the scalar field vanishes at the point of the transition between the Higgs phase and the symmetric phase. Our analysis shows that at the point where the scalar field condensate disappears, lattice M_H does not vanish. However, it may vanish, in principle, at some other point. If both M_Z and M_H vanish simultaneously at γ_{c0} , at this point the model becomes scale invariant and the formal continuum limit of the lattice model can be achieved at γ_{c0} . This point may then appear as the point of the second order phase transition. Near γ_{c0} the fluctuations of the gauge boson correlator are strong and at the present moment we do not make definite conclusions on the behavior of the system at γ_{c0} . However, the calculated susceptibilities do not have peaks at this point, which is an indirect indication that the real second order phase transition cannot appear at γ_{c0} . It is worth mentioning that within the region (γ_{c0}, γ_c) the scalar field is not condensed. That is why we guess this region has nothing to do with real continuum physics.

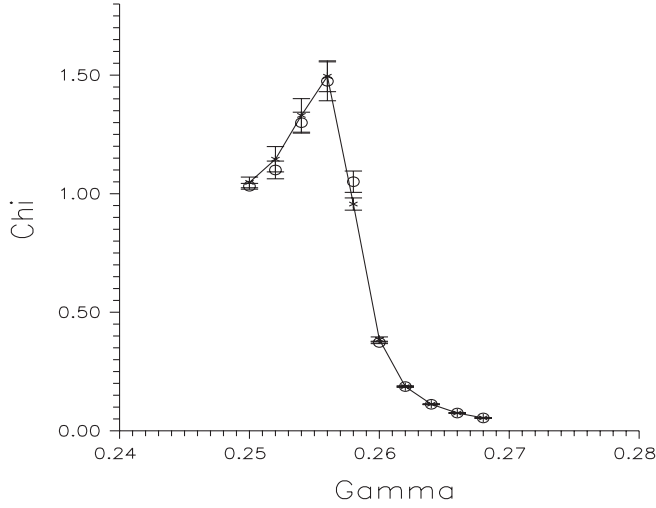


FIG. 2. Susceptibility $\chi = \langle H^2 \rangle - \langle H \rangle^2$ (for $H_x = \sum_y Z_{xy}^2$) as a function of γ at $\lambda = 0.001$ and $\beta = 12$. Circles correspond to the lattice $12^3 \times 16$. Crosses correspond to the lattice $8^3 \times 16$.

We investigated carefully the region $\gamma \geq \gamma_c$ for $\lambda = 0.001, 0.0025, 0.009$. We observe that for $\gamma_c < \gamma < \gamma_{c2}$ Nambu monopoles dominate the vacuum and the usual perturbation theory cannot be applied. For this reason, most likely, the interval (γ_c, γ_{c2}) also has no connection with the conventional continuum electroweak theory. At the same time for $\gamma \gg \gamma_{c2}$ the behavior of the system is close to what one would expect based on the usual perturbative continuum Weinberg-Salam model. It is worth mentioning that the value of the renormalized Higgs boson mass does not deviate significantly from its bare value near the transition point γ_c . For example, for λ around 0.009 and $\gamma = 0.274$ bare value of the Higgs mass is around 270 GeV, while the observed renormalized value is 300 ± 70 GeV.

VI. EFFECTIVE CONSTRAINT POTENTIAL

We have calculated the constraint effective potential for $|\Phi|$ using the histogram method. The calculations have been performed on the lattice $8^3 \times 16$. The probability $h(\phi)$ to find the value of $|\Phi|$ within the interval $[\phi - 0.05; \phi + 0.05]$ has been calculated for $\phi = 0.05 + N * 0.1$, $N = 0, 1, 2, \dots$. This probability is related to the effective potential as $h(\phi) = \phi^3 e^{-V(\phi)}$. That is why we extract the potential from $h(\phi)$ as

$$V(\phi) = -\log h(\phi) + 3 \log \phi. \quad (20)$$

(See Fig. 3.) It is worth mentioning that $h(0.05)$ is calculated as the probability to find the value of $|\Phi|$ within the interval $[0; 0.1]$. Within this interval $\log \phi$ is ill defined. That is why we exclude the point $\phi = 0.05$ from our data. Instead we calculate $V(0)$ using the extrapolation of the data at $0.15 \leq \phi \leq 2.0$. The extrapolation is performed

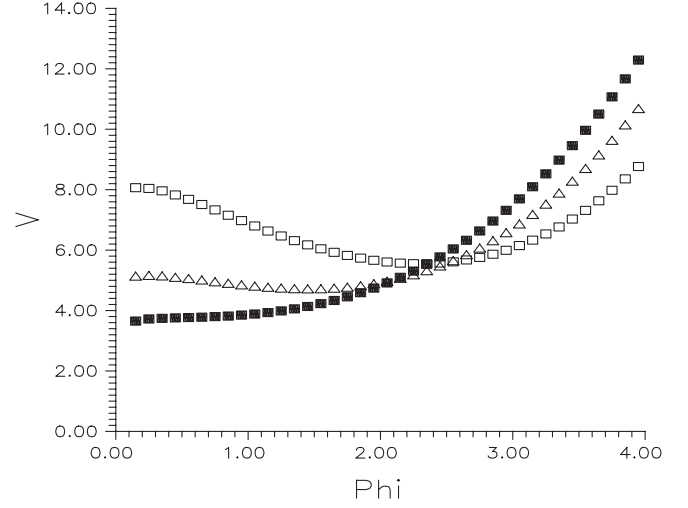


FIG. 3. The effective constraint potential at $\lambda = 0.009$ and $\beta = 12$. Solid squares correspond to $\gamma_c = 0.273$. Empty squares correspond to $\gamma = 0.29$. Triangles correspond to $\gamma = 0.279$. The error bars are about the same size as the symbols used.

using the polynomial fit with the powers of ϕ up to the third (average deviation of the fit from the data is around 1 percent). Next, we introduce the useful quantity $H = V(0) - V(\phi_m)$, which is called the potential barrier height (here ϕ_m is the point where V achieves its minimum).

As an example we represent in Fig. 4 the values of ϕ_m for $\lambda = 0.001$, $\beta = 12$. In Fig. 5 we represent the values of H for $\lambda = 0.009$, $\beta = 12$. One can see that the values of ϕ_m and H increase when γ is increased. The maximum of the susceptibility constructed of the Higgs field creation operator $H_x = \sum_y Z_{xy}^2$ (see, for example, Fig. 2) coincides with the point where ϕ_m vanishes within the statistical errors. We localize the position of the transition points at the points where ϕ_m vanishes: $\gamma_c = 0.274 \pm 0.001$ at

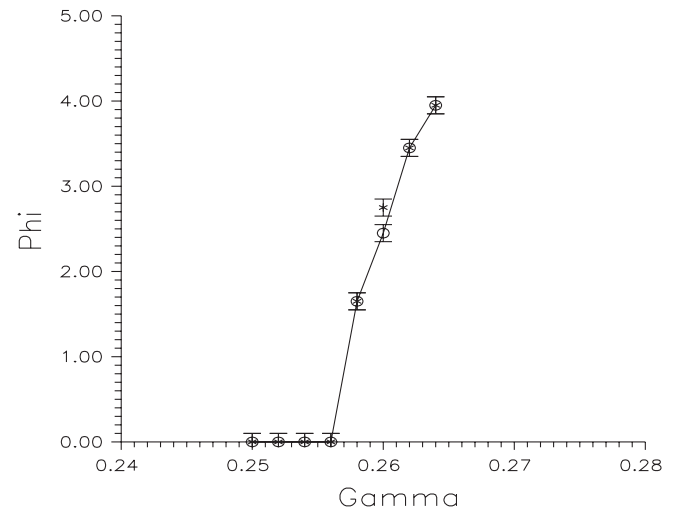


FIG. 4. ϕ_m as a function of γ at $\lambda = 0.001$ and $\beta = 12$. Circles correspond to lattice $8^3 \times 16$. Crosses correspond to lattice $12^3 \times 16$.

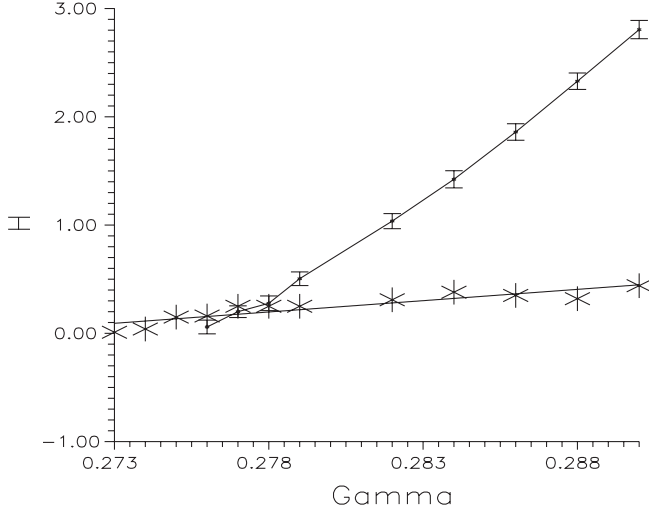


FIG. 5. H (points) vs H_{fluct} (stars) as a function of γ at $\lambda = 0.009$ and $\beta = 12$. Statistical errors for H_{fluct} are about the same size as the symbols used.

$\lambda = 0.009$, $\gamma_c = 0.26 \pm 0.001$ at $\lambda = 0.0025$, and $\gamma_c = 0.256 \pm 0.001$ at $\lambda = 0.001$.

The maximum of the scalar field fluctuation (see, for example, Fig. 6) is shifted to larger values of γ than the transition point. Again we do not observe any difference in $\delta\phi$ for the considered lattice sizes. This also indicates that the transition at these values of λ is a crossover.

It is important to understand which value of barrier height can be considered as small and which value can be considered as large. Our suggestion is to compare $H = V(0) - V(\phi_m)$ with $H_{\text{fluct}} = V(\phi_m + \delta\phi) - V(\phi_m)$, where $\delta\phi$ is the fluctuation of $|\Phi|$. From Fig. 5 it is clear that there exists the value of γ (we denote it γ_{c2}) such that at $\gamma_c < \gamma < \gamma_{c2}$ the barrier height H is of the order of H_{fluct} while for $\gamma_{c2} \ll \gamma$ the barrier height is essentially larger than H_{fluct} . The rough estimate for this pseudocritical value is $\gamma_{c2} \sim 0.278$ at $\lambda = 0.009$.

The fluctuations of $|\Phi|$ are around $\delta\phi \sim 0.6$ for all considered values of γ at $\lambda = 0.009, 0.0025, 0.001$, $\beta = 12$. It follows from our data (see also Fig. 7) that $\phi_m, \langle|\phi|\rangle \gg \delta\phi$ at $\gamma_{c2} \ll \gamma$ while $\phi_m, \langle|\phi|\rangle \sim \delta\phi$ at $\gamma_{c2} > \gamma$. Based on these observations we expect that in the region $\gamma_{c2} \ll \gamma$ the usual perturbation expansion around the trivial vacuum of spontaneously broken theory can be applied to the lattice Weinberg-Salam model while in the FR $\gamma_c < \gamma < \gamma_{c2}$ it cannot be applied. In the same way we define the pseudocritical value γ_{c2} at $\lambda = 0.001, 0.0025$. Namely, $\gamma_{c2} \sim 0.278$ for $\lambda = 0.009$; ~ 0.262 for $\lambda = 0.0025$; ~ 0.258 for $\lambda = 0.001$.

VII. THE RENORMALIZED COUPLING

In order to calculate the renormalized fine structure constant $\alpha_R = e^2/4\pi$ (where e is the electric charge), we use the potential for infinitely heavy external fermions.

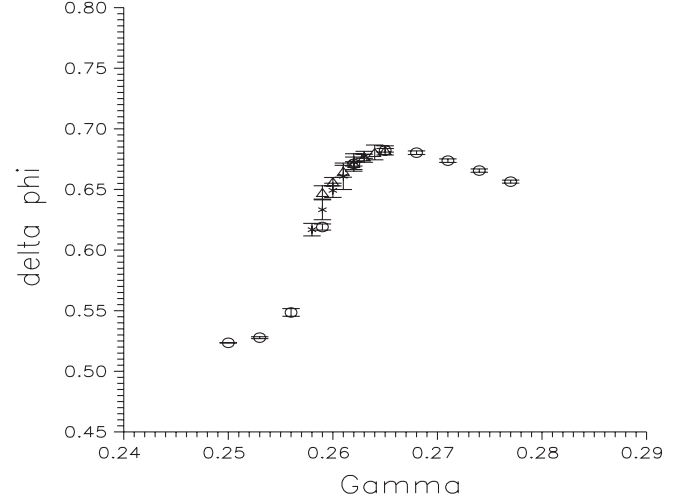


FIG. 6. Fluctuation $\delta\phi$ as a function of γ at $\lambda = 0.0025$ and $\beta = 12$. Circles correspond to the lattice $8^3 \times 16$. Crosses correspond to the lattice $12^3 \times 16$. Triangles correspond to the lattice 16^4 . The transition point is $\gamma_c = 0.261 \pm 0.001$; it is clear that the maximum of $\delta\phi$ is shifted to larger values of γ .

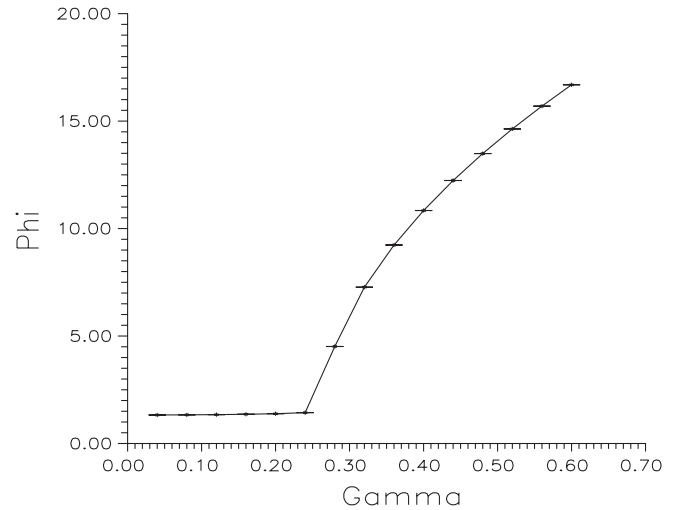


FIG. 7. Mean value of $|\phi|$ as a function of γ at $\lambda = 0.0025$ and $\beta = 12$. (Lattice $8^3 \times 16$.)

We consider Wilson loops for the right-handed external leptons:

$$\mathcal{W}_{\text{lept}}^R(l) = \langle \text{Re} \Pi_{(xy) \in l} e^{2i\theta_{xy}} \rangle. \quad (21)$$

Here l denotes a closed contour on the lattice. We consider the following quantity constructed from the rectangular Wilson loop of size $r \times t$:

$$\mathcal{V}(r) = \log \lim_{t \rightarrow \infty} \frac{\mathcal{W}(r \times t)}{\mathcal{W}(r \times (t+1))}. \quad (22)$$

Because of the exchange by virtual photons at large enough distances, we expect the appearance of the Coulomb interaction

$$\mathcal{V}(r) = -\frac{\alpha_R}{r} + \text{const.} \quad (23)$$

It should be mentioned here that in order to extract the renormalized value of α one may apply to \mathcal{V} the fit obtained using the Coulomb interaction in momentum space. The lattice Fourier transform then gives

$$\mathcal{U}(r) = -\alpha_R \mathcal{U}(r) + \text{const},$$

$$\mathcal{U}(r) = \frac{\pi}{N^3} \sum_{\vec{p} \neq 0} \frac{e^{i\vec{p}_3 r}}{\sin^2 p_1/2 + \sin^2 p_2/2 + \sin^2 p_3/2}. \quad (24)$$

Here N is the lattice size, $p_i = \frac{2\pi}{L} k_i$, $k_i = 0, \dots, L-1$. On large enough lattices at $r \ll L$ both definitions approach each other. On the lattices we use, the values of the renormalized α_R extracted from (23) and (24) are essentially different from each other. Either of the two ways, (23) or (24), may be considered as the definition of the renormalized α on the finite lattice. And there is no particular reason to prefer the potential defined using the lattice Fourier transform of the Coulomb law in momentum space. Actually, our study shows that the single $1/r$ fit approximates \mathcal{V} much better. Moreover, the values of renormalized α calculated using this fit are essentially closer to the tree level estimate than those calculated using the fit (24).

In practice instead of (22) we use the potential that depends on additional parameter T :

$$\mathcal{V}(r, T) = \log \frac{W(r \times T)}{W(r \times (T+1))}. \quad (25)$$

For example, on the lattice 16^4 the values $T = 4, 5, 6, 7, 8$ are used; on the lattice $12^3 \times 16$ the values $T = 4, 5, 6$ are used; on the lattice $8^3 \times 16$ the value $T = 4$ is used. As a result $\alpha_R = \alpha_R(T)$ may depend both on the lattice size and on T . The dependence on T was missed in [4] (where for lattices $12^3 \times 16$, 16^4 we used $T = 5$, while for the lattice $8^3 \times 16$ we used $T = 4$).

In Fig. 8 we represent as an example the dependence of the potential for $T = 8$ on $1/R$. As already mentioned (23) approximates the potential much better than (24). Therefore we used the fit (23) to extract α_R . This should be compared with the results of [21], where for similar reasons the single $e^{-\mu r}/r$ fit (instead of the lattice Yukawa fit) was used in order to determine the renormalized coupling constant in the $SU(2)$ gauge-Higgs model.

Because of the dependence of $\alpha_R(T)$ on T there is the essential uncertainty in the definition of α_R related to finite volume effects. For example, at $\gamma = 0.29$, $\lambda = 0.009$, and $\beta = 12$, the value of α_R calculated on the lattice 16^4 varies between $\alpha_R(4) \sim 1/(93 \pm 1)$ and $\alpha_R(8) \sim 1/(108 \pm 2)$ [at the same time on the lattice $8^3 \times 16$ the value is $\alpha_R(4) = 1/(100 \pm 1)$]. At $\gamma = 0.274$, $\lambda = 0.009$, and $\beta = 12$, the value of α_R calculated on the lattice $20^3 \times 24$ varies between $\alpha_R(4) \sim 1/(98 \pm 1)$ and $\alpha_R(10) = 1/(106 \pm 1)$ [at the same time on the lattice $8^3 \times 16$ the

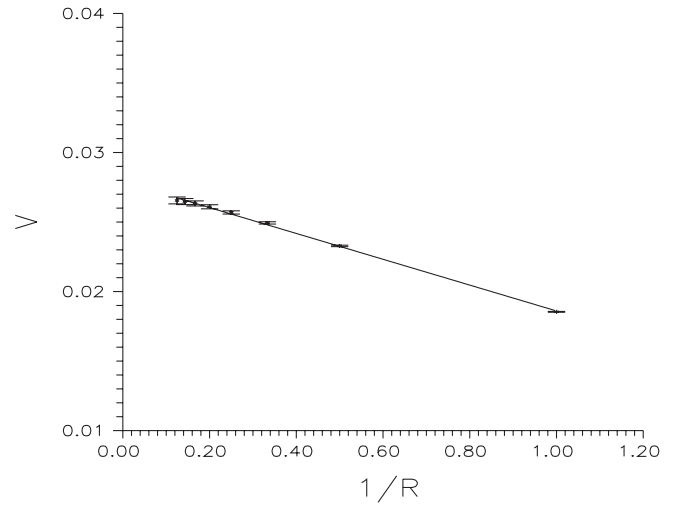


FIG. 8. The potential ($T = 8$) for the right-handed leptons vs $1/R$ at $\gamma = 0.262$, $\lambda = 0.0025$, and $\beta = 12$ (lattice 16^4).

value is $\alpha_R(4) = 1/(99 \pm 1)$]. Below for the lattice $8^3 \times 16$ we use $T = 4$, for the lattice $12^3 \times 16$ we use $T = 6$, and for the lattice 16^4 we use $T = 8$. Therefore, the dependence on T is absorbed into the dependence on the lattice size. As an example, in Fig. 9 we represent the renormalized fine structure constant [calculated using the fit (23)] at $\lambda = 0.0025$, $\beta = 12$. The calculated values are to be compared with bare constant $\alpha_0 = 1/(4\pi\beta) \sim 1/150$ at $\beta = 12$. One can see that for $\gamma \gg \gamma_{c2}$ the tree level estimate is approached slowly while within the FR the renormalized α differs essentially from the tree level estimate. This is in correspondence with our supposition that the perturbation theory cannot be valid within the FR while

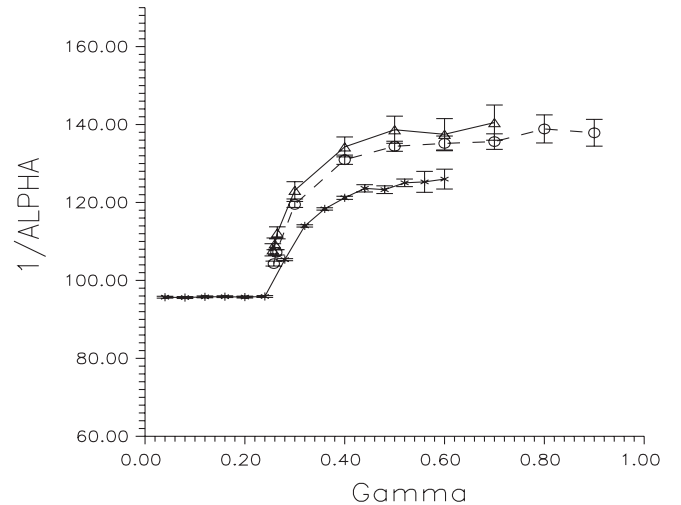


FIG. 9. The inverse renormalized fine structure constant as a function of γ at $\lambda = 0.0025$ and $\beta = 12$. It slowly approaches the tree level estimate ~ 150 when γ and the lattice size are increased. Circles correspond to lattice $12^3 \times 16$. Crosses correspond to lattice $8^3 \times 16$. Triangles correspond to lattice 16^4 .

it works well far from the FR. The dependence of α_R on the lattice size is clear: for the larger lattices α_R approaches its tree level estimate faster than for the smaller ones. Unfortunately, due to the difficulties in simulation of the system at large γ we cannot observe this pattern in detail. At the present moment the value of α_R most close to the tree level estimate is obtained on the lattice $12^3 \times 16$ and is about $1/140$ (at $\lambda = 0.0025, 0.001$; $\beta = 12$; $\gamma \sim 1$).

VIII. MASSES AND THE LATTICE SPACING

After fixing the unitary gauge $\Phi_1 \in R$, $\Phi_2 = 0$, $\Phi_1 \geq 0$, the following variables are considered as creating a Z boson and a W boson, respectively:

$$\begin{aligned} Z_{xy} &= Z_x^\mu = -\sin[\text{Arg}(U_{xy}^{11} e^{i\theta_{xy}})], \\ W_{xy} &= W_x^\mu = U_{xy}^{12} e^{-i\theta_{xy}}. \end{aligned} \quad (26)$$

Here, μ represents the direction (xy) . The electromagnetic $U(1)$ symmetry remains:

$$U_{xy} \rightarrow g_x^\dagger U_{xy} g_y, \quad \theta_{xy} \rightarrow \theta_{xy} - \alpha_y/2 + \alpha_x/2, \quad (27)$$

where $g_x = \text{diag}(e^{i\alpha_x/2}, e^{-i\alpha_x/2})$. There exists a $U(1)$ lattice gauge field, which is defined as

$$A_{xy} = A_x^\mu = [-\text{Arg} U_{xy}^{11} + \theta_{xy}] \bmod 2\pi, \quad (28)$$

that transforms as $A_{xy} \rightarrow A_{xy} - \alpha_y + \alpha_x$. The field W transforms as $W_{xy} \rightarrow W_{xy} e^{-i\alpha_x}$.

The W -boson field is charged with respect to the $U(1)$ symmetry. Therefore we fix the lattice Landau gauge in order to investigate the W -boson propagator. The lattice Landau gauge is fixed via minimizing [with respect to the $U(1)$ gauge transformations] the following functional:

$$F = \sum_{xy} (1 - \cos(A_{xy})). \quad (29)$$

Then we extract the mass of the W boson from the correlator

$$\frac{1}{N^6} \sum_{\vec{x}, \vec{y}} \left\langle \sum_{\mu} W_x^\mu (W_y^\mu)^\dagger \right\rangle \sim e^{-M_W |x_0 - y_0|} + e^{-M_W (L - |x_0 - y_0|)}. \quad (30)$$

Here the summation $\sum_{\vec{x}, \vec{y}}$ is over the three “space” components of the four-vectors x and y , while x_0, y_0 denote their “time” components. N is the lattice length in the space direction. L is the lattice length in the time direction.

In order to evaluate the masses of the Z boson and the Higgs boson we use the correlators:

$$\frac{1}{N^6} \sum_{\vec{x}, \vec{y}} \left\langle \sum_{\mu} Z_x^\mu Z_y^\mu \right\rangle \sim e^{-M_Z |x_0 - y_0|} + e^{-M_Z (L - |x_0 - y_0|)} \quad (31)$$

and

$$\frac{1}{N^6} \sum_{\vec{x}, \vec{y}} (\langle H_x H_y \rangle - \langle H \rangle^2) \sim e^{-M_H |x_0 - y_0|} + e^{-M_H (L - |x_0 - y_0|)}. \quad (32)$$

In lattice calculations we used two different operators that create Higgs bosons: $H_x = |\Phi|$ and $H_x = \sum_y Z_{xy}^2$. In both cases H_x is defined at the site x , the sum \sum_y is over its neighboring sites y .

The physical scale is given in our lattice theory by the value of the Z -boson mass $M_Z^{\text{phys}} \sim 91$ GeV. Therefore the lattice spacing is evaluated to be $a \sim [91 \text{ GeV}]^{-1} M_Z$, where M_Z is the Z -boson mass in lattice units. Similar calculations have been performed in [3] for $\lambda = \infty$. It has been found that the W -boson mass contains an artificial dependence on the lattice size. We suppose that this dependence is due to the photon cloud surrounding the W boson. The energy of this cloud is related to the renormalization of the fine structure constant. Therefore the Z -boson mass was used in order to fix the scale.

Our data show that $\Lambda = \frac{\pi}{a} = (\pi \times 91 \text{ GeV})/M_Z$ is increased slowly with the decrease of γ at any fixed λ . We investigated carefully the vicinity of the transition point at fixed $\lambda = 0.001, 0.0025, 0.009$ and $\beta = 12$. It has been found that at the transition point the value of Λ is equal to 1.4 ± 0.2 TeV for $\lambda = 0.009, 0.0025, 0.001$. A check of the dependence on the lattice size ($8^3 \times 16, 12^3 \times 16, 16^4, 20^3 \times 24$ at $\lambda = 0.009$; $8^3 \times 16, 12^3 \times 16, 16^4$ at $\lambda = 0.0025$; $8^3 \times 16, 12^3 \times 16$ at $\lambda = 0.001$) does not show an essential dependence of this value on the lattice size. This is illustrated by Figs. 10–12. From these figures it also follows that at the value of γ equal to γ_{c2} (~ 0.278 for $\lambda = 0.009$; ~ 0.262 for $\lambda = 0.0025$; ~ 0.258 for $\lambda = 0.001$) the calculated value of the cutoff is about 1 TeV.

It is worth mentioning that the linear fit applied (in some vicinity of γ_c) to the dependence of M_Z on γ predicts the vanishing of $M_Z(\gamma)$ at γ equal to $\gamma_{c0} < \gamma_c$. Within the statistical errors $\gamma_{c0} = 0.253 \pm 0.001$ for $\lambda = 0.001$, $\gamma_{c0} = 0.253 \pm 0.001$ for $\lambda = 0.0025$, $\gamma_{c0} = 0.254 \pm 0.001$ for $\lambda = 0.009$. We perform direct calculations within the region (γ_{c0}, γ_c) at $\lambda = 0.001, 0.0025$. These calculations show that the fluctuations of the correlator (31) are increased (compared with the values of the correlator) fast when γ is decreased. Already for $\gamma = 0.255$ at $\lambda = 0.0025$ ($\gamma_c = 0.26$) and for $\gamma = 0.254$ at $\lambda = 0.001$ ($\gamma_c = 0.258$), the values of the correlator at $|x_0 - y_0| > 0$ are smaller than the statistical errors. Most likely, at $\gamma \leq \gamma_{c0}$ it is necessary to apply another gauge [like in the pure $SU(2) \times U(1)$ gauge model] in order to calculate gauge boson propagators. At the present moment we do not estimate the scalar particle mass at γ_{c0} because of the lack of statistics. The behavior of the other quantities is smooth at $\gamma \sim \gamma_{c0}$; no maximum of $\delta\phi$ or other susceptibilities is observed there (see, for example, Fig. 2). Based on our data it is natural to suppose that the lattice gauge boson mass may vanish at $\gamma \sim \gamma_{c0}$, although we do not

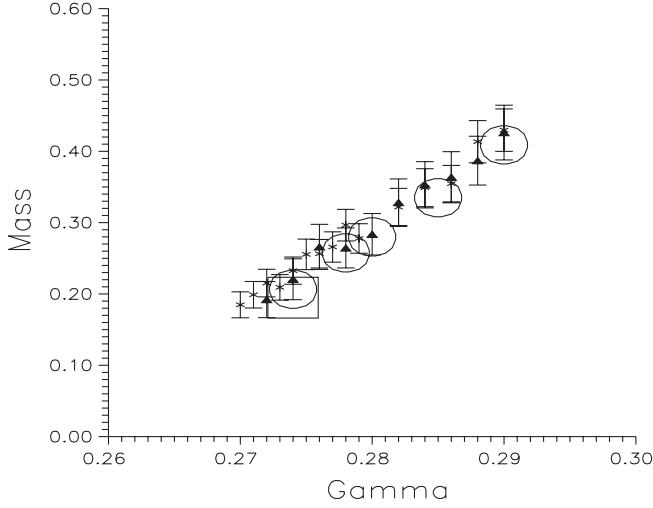


FIG. 10. Z-boson mass in lattice units at $\lambda = 0.009$ and $\beta = 12$ as a function of γ . Solid triangles correspond to lattice $12^3 \times 16$. Crosses correspond to lattice $8^3 \times 16$. Circles correspond to lattice 16^4 . Square corresponds to lattice $20^3 \times 24$. (The error bars for lattices $16^3 \times 16$ and $20^3 \times 24$ are about the same size as the symbols used.)

observe the correspondent pattern in detail because of the strong fluctuations of the correlator (31) near γ_{c0} . As mentioned above, the transition for the considered values of couplings is, most likely, a crossover. There are 3 exceptional points: γ_{c0} , where the lattice value of M_Z may vanish, γ_c , where the scalar field condensate disappears, and γ_{c2} , which denotes the boundary of the fluctuational region. This situation is typical for the crossovers: different quantities change their behavior at different points on the phase diagram. At the present moment we do not exclude that the second order phase transition may take place at

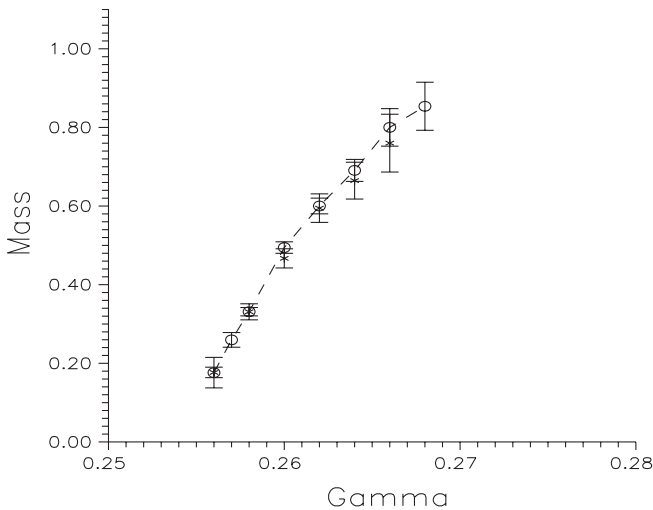


FIG. 11. Z-boson mass in lattice units at $\lambda = 0.001$ and $\beta = 12$. Circles correspond to lattice $8^3 \times 16$. Crosses correspond to lattice $12^3 \times 16$.

γ_{c0} . This would happen if both mass parameters (Z-boson mass and scalar particle mass) vanish simultaneously at this point. The careful investigation of the vicinity of γ_{c0} is to be the subject of further research.

In the Higgs channel the situation is more difficult. Because of the lack of statistics we cannot estimate the masses in this channel using the correlators (32) at all considered values of coupling constants. Moreover, at several points, where we have estimated the renormalized Higgs boson mass, the statistical errors are much larger than that of for the Z-boson mass. At the present moment we can represent the data at four points on the lattice $8^3 \times 16$: ($\gamma = 0.274$, $\lambda = 0.009$, $\beta = 12$), ($\gamma = 0.290$, $\lambda = 0.009$, $\beta = 12$), ($\gamma = 0.261$, $\lambda = 0.0025$, $\beta = 12$), and ($\gamma = 0.257$, $\lambda = 0.001$, $\beta = 12$).

The first point roughly corresponds to the position of the transition at $\lambda = 0.009$, $\beta = 12$, while the second point is situated deep within the Higgs phase. These two points correspond to bare Higgs mass around 270 GeV. At the point ($\gamma = 0.274$, $\lambda = 0.009$, $\beta = 12$) we have collected enough statistics to calculate the correlator (32) up to the time separation $|x_0 - y_0| = 4$. The value $\gamma = 0.274$ corresponds roughly to the position of the phase transition. We estimate at this point $M_H = 300 \pm 40$ GeV. At the point ($\gamma = 0.29$, $\lambda = 0.009$, $\beta = 12$), we calculate the correlator with reasonable accuracy up to $|x_0 - y_0| = 3$. At this point $M_H = 265 \pm 70$ GeV.

For $\lambda = 0.001$, 0.0025 we calculate the Higgs boson mass close to the transition points. Similar to the case $\lambda = 0.009$ we do not observe here essential deviation from the tree level estimates. Namely, for $\lambda = 0.001$, $\gamma = 0.257$ we have $M_H = 90 \pm 20$ GeV (tree level value is $M_H^0 \sim 100$ GeV). For this point we have collected enough statistics to calculate correlator (32) up to the time separation

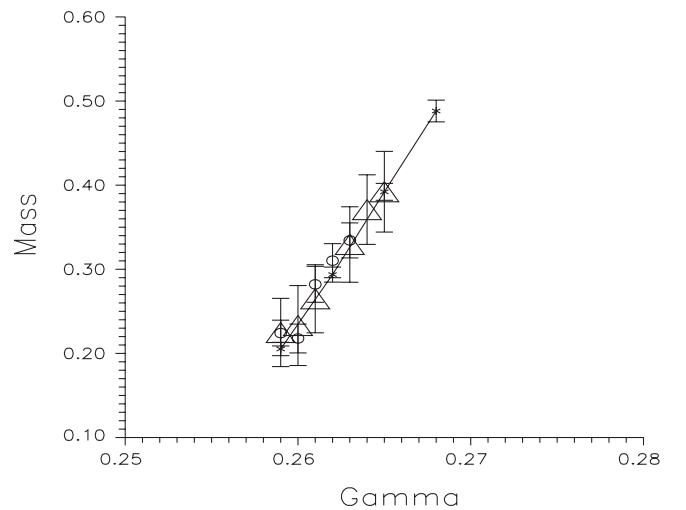


FIG. 12. Z-boson mass in lattice units at $\lambda = 0.0025$ and $\beta = 12$. Circles correspond to lattice $12^3 \times 16$. Crosses correspond to lattice $8^3 \times 16$. Triangles correspond to lattice 16^4 .

$|x_0 - y_0| = 8$. For $\lambda = 0.0025$, $\gamma = 0.261$ we have $M_H = 170 \pm 30$ GeV (tree level value is $M_H^0 \sim 150$ GeV). For this point we have collected enough statistics to calculate correlator (32) up to the time separation $|x_0 - y_0| = 4$. It is worth mentioning that in order to calculate the Z-boson mass we fit correlator (31) for $8 \geq |x_0 - y_0| \geq 1$.

IX. NAMBU MONOPOLE DENSITY

The worldlines of the quantum Nambu monopoles can be extracted from the field configurations according to Eq. (17). The monopole density is defined as

$$\rho = \left\langle \frac{\sum_{\text{links}} |j_{\text{link}}|}{4V^L} \right\rangle,$$

where V^L is the lattice volume.

In Figs. 13–15 we represent Nambu monopole density as a function of γ at $\lambda = 0.009, 0.0025, 0.001$, $\beta = 12$. The value of monopole density at γ_c is around 0.1.

According to the classical picture the Nambu monopole size is of the order of M_H^{-1} . Therefore, for example, for $a^{-1} \sim 430$ GeV and $M_H \sim 300, 150, 100$ GeV, the expected size of the monopole is about a lattice spacing. The monopole density around 0.1 means that among 10 sites there exist 4 sites that are occupied by the monopole. Average distance between the two monopoles is, therefore, less than 1 lattice spacing and it is not possible at all to speak of the given configurations as representing the physical Nambu monopole.

At $\gamma = \gamma_{c2}$ the Nambu monopole density is of the order of 0.01. This means that among about 25 sites there exists

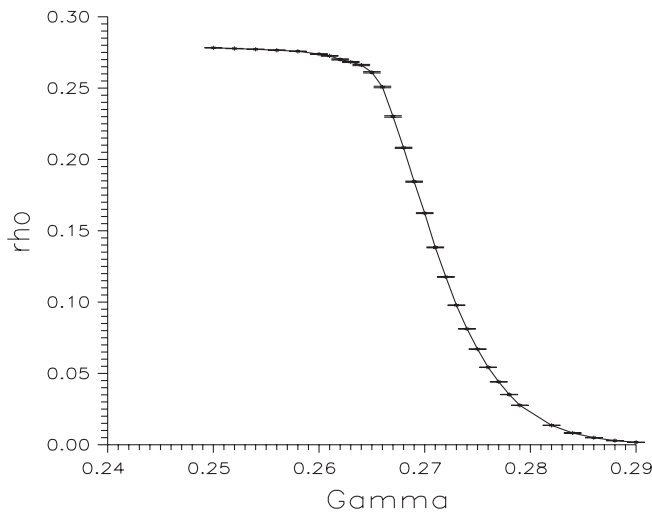


FIG. 13. Nambu monopole density as a function of γ at $\lambda = 0.009$ and $\beta = 12$. (Lattice $8^3 \times 16$.)

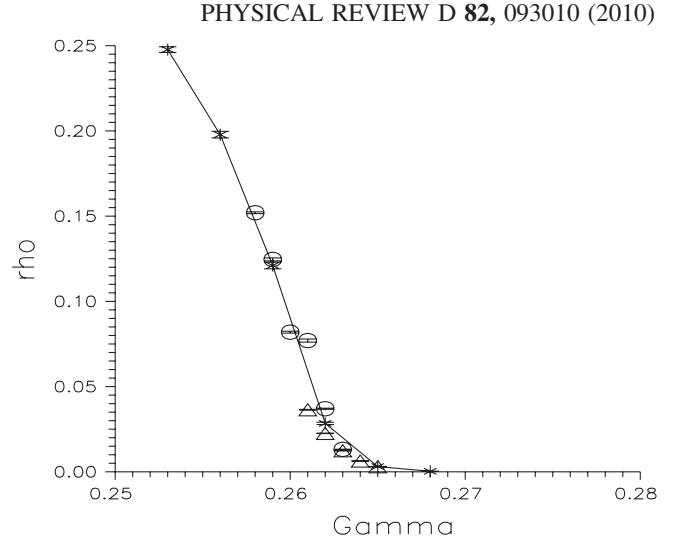


FIG. 14. Nambu monopole density as a function of γ at $\lambda = 0.0025$ and $\beta = 12$. Circles correspond to lattice $12^3 \times 16$. Crosses correspond to lattice $8^3 \times 16$. Triangles correspond to lattice 16^4 .

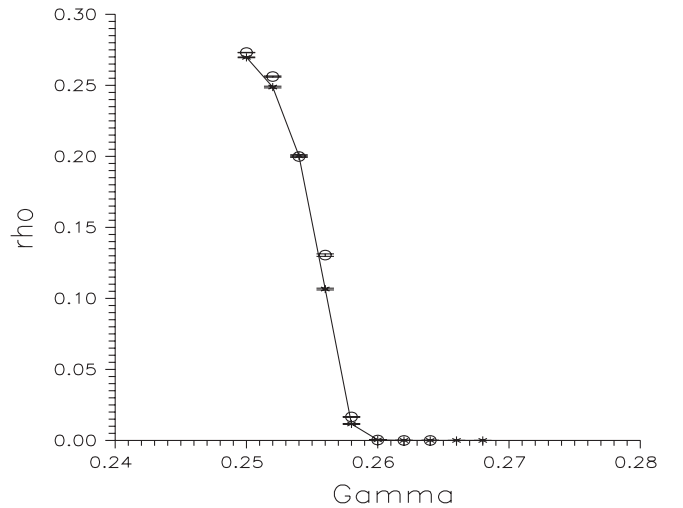


FIG. 15. Nambu monopole density as a function of γ at $\lambda = 0.001$ and $\beta = 12$. Circles correspond to lattice $12^3 \times 16$. Crosses correspond to lattice $8^3 \times 16$.

one site that is occupied by the monopole. Average distance between the two monopoles is, therefore, between one and two lattice spacings. We see that at this value of γ the average distance between Nambu monopoles is of the order of their size.

We summarize the above observations as follows. Within the fluctuational region the configurations under consideration do not represent single Nambu monopoles. Instead these configurations can be considered as the collection of monopolelike objects that is so dense that the average distance between the objects is of the order of their

size. On the other hand, at $\gamma \gg \gamma_{c2}$ the considered configurations do represent single Nambu monopoles and the average distance between them is much larger than their size. In other words out of the FR vacuum can be treated as a gas of Nambu monopoles, while within the FR vacuum can be treated as a liquid composed of monopolelike objects.

It is worth mentioning that somewhere inside the Z string connecting the classical Nambu monopoles the Higgs field is zero: $|\Phi| = 0$. This means that the Z string with the Nambu monopoles at its ends can be considered as an embryo of the symmetric phase within the Higgs phase. We observe that the density of these embryos is increased when the phase transition is approached. Within the fluctuational region the two phases are mixed, which is related to the large value of Nambu monopole density.

That is why we come to the conclusion that the vacuum of the lattice Weinberg-Salam model within the FR has nothing to do with the continuum perturbation theory. This means that the usual perturbation expansion around the trivial vacuum [gauge field equal to zero, the scalar field equal to $(\phi_m, 0)^T$] cannot be valid within the FR. This might explain why we do not observe in our numerical simulations the large values of Λ predicted by the conventional perturbation theory.

X. CONCLUSIONS

In the present paper we demonstrate that while approaching continuum physics in the lattice Weinberg-Salam model one encounters the nonperturbative effects. Namely, the continuum physics is to be approached in the vicinity of the transition between the physical Higgs phase and the symmetric phase of the model (in the symmetric phase the scalar field is not condensed). The ultraviolet cutoff is increased when the transition point is approached along the line of constant physics. There exists the FR on the phase diagram of the lattice Weinberg-Salam model. This region is situated in the vicinity of the transition between the Higgs phase and the symmetric phase (where scalar field is not condensed). According to our data this transition is, most likely, a crossover. We localize its position at the point $\gamma_c(\lambda, \beta, \theta_W)$, where the scalar field condensate disappears. We calculate the effective constraint potential $V(\phi)$ for the Higgs field. It has a minimum at the nonzero value ϕ_m in the physical Higgs phase. At the considered values of λ, β, θ_W for γ between γ_c and γ_{c2} (γ_{c2} is in the Higgs phase), the fluctuations of the scalar field become of the order of ϕ_m . Moreover, the “barrier height” $H = V(0) - V(\phi_m)$ is of the order of $V(\phi_m + \delta\phi) - V(\phi_m)$, where $\delta\phi$ is the fluctuation of $|\Phi|$. Therefore, we refer to this region as FR.

The scalar field must be equal to zero somewhere within the classical Nambu monopole. That is why this object can be considered as an embryo of the unphysical symmetric phase within the physical Higgs phase of the model. We

investigate properties of the quantum Nambu monopoles. Within the FR they are so dense that the average distance between them becomes of the order of their size. This means that the two phases are mixed within the FR. All these results show that the vacuum of the lattice Weinberg-Salam model in the FR is essentially different from the trivial vacuum used in the conventional perturbation theory. As a result the use of the perturbation theory in this region is limited.

Our numerical results show that at M_H around 270, 150, 100 GeV and the bare fine structure constant around $1/150$ the maximal value of the cutoff admitted out of the FR for the considered lattice sizes cannot exceed the value around 1 TeV. Within the FR the larger values of the cutoff can be achieved in principle. The maximum for the value of the cutoff Λ_c within the Higgs “phase” of the lattice model is achieved at the point of the transition to the region of the phase diagram, where the scalar field is not condensed. Our estimate for this value is $\Lambda_c = 1.4 \pm 0.2$ TeV for the considered lattice sizes. Far from the fluctuational region the behavior of the lattice model in general is close to what we expect based on the continuous perturbation theory. As already mentioned, at the considered values of couplings the transition is, most likely, a crossover. This follows from the observation that various quantities (Z -boson mass, the fluctuation of the scalar field, etc.) do not depend on the lattice size at the transition point. Within the symmetric “phase” of the lattice model (where the scalar field is not condensed) in some vicinity of the transition between this phase and the Higgs phase (where the scalar field is condensed), the lattice gauge boson masses do not vanish. The statistical error for M_Z is increased fast when γ is decreased starting from the pseudocritical value γ_c . At $\gamma \leq \gamma_{c0} < \gamma_c$ (within the symmetric phase) the values of the Z -boson correlator (31) are smaller than the statistical errors. Therefore, our procedure cannot give the values of gauge boson masses in this region. Most likely, here the other gauge is to be applied in order to calculate gauge boson propagators (we used in our simulations the unitary gauge). It is worth mentioning that the perturbation theory predicts zero gauge boson masses within the symmetric phase. Most likely, this prediction fails within the interval (γ_{c0}, γ_c) due to nonperturbative effects.

An important question is how to treat finite volume effects that are present in all observables that contain long-range electromagnetic Coulomb interactions. In particular, we see that these effects are strong in the renormalized fine structure constant (about 10% when the lattice size varies from $8^3 \times 16$ to 16^4) and in the mass of the electrically charged W boson. On the other hand all observables related to the $SU(2)$ constituent of the model do not possess essential dependence on the lattice size. In particular, the Z -boson mass M_Z (and the cutoff Λ), density ρ_{Nambu} of Nambu monopoles [30], fluctuation of the scalar field $\delta\phi$, as well as the position of the transition

between the phases of the lattice model practically do not depend on the lattice size. Our point of view is that the influence of long-range electromagnetic interactions on these observables is negligible compared to their tree level and nonperturbative constituents. Actually, electromagnetic interactions can be taken into account perturbatively, with the renormalized $\alpha \sim 1/100$ as the parameter of the perturbation expansion. This was the reason why in the previous numerical studies of the $SU(2)$ gauge-Higgs model the $U(1)$ constituent of the Weinberg-Salam model was completely disregarded [8–21]. To summarize, we suppose that in spite of the presence of finite volume effects in the fine structure constant and W -boson mass, the calculated values of M_Z , Λ , ρ_{Nambu} , $\delta\phi$, etc., can be considered as free of these effects [31] (up to the perturbations suppressed by the factor $\alpha \sim 1/100$).

Based on our data it is natural to suppose that the lattice gauge boson mass may vanish at $\gamma \sim \gamma_{c0}$, although we do not observe the correspondent pattern in detail because of the strong fluctuations of the correlator (31) near γ_{c0} . If so, there exist 3 pseudocritical points: γ_{c0} , where the lattice value of M_Z vanishes [at this point the cutoff calculated as $\Lambda = (\pi \times 91 \text{ GeV})/M_Z$ tends to infinity], γ_c , where scalar field condensate disappears, and γ_{c2} , which denotes the boundary of the fluctuational region (at $\gamma \sim \gamma_{c2}$ the average distance between Nambu monopoles becomes of the order of their size). This situation is typical for the crossovers: different quantities change their behavior at different points on the phase diagram. There still exists the possibility that the point γ_{c0} corresponds to the second

order phase transition (this may happen if, in addition, the scalar particle mass vanishes at γ_{c0}). However, the absence of a peak in the scalar field fluctuation and in susceptibility (19) at this point indicates that this is a crossover. Actually, this possibility is to be checked carefully but this is to be a subject of another work. There is an important question: what is the relation between the conventional electroweak physics and the regions (γ_{c0}, γ_c) and (γ_c, γ_{c2}) ? Our expectation is that both these regions have nothing to do with real continuum physics. For the first region this is more or less obvious: there the scalar field is not condensed that contradicts with the usual spontaneous breakdown pattern. As for the second region, the situation is not so obvious. However, there the nonperturbative effects are strong and the Nambu monopoles dominate the vacuum that seems to us unphysical. With all the mentioned above we come to the conclusion that our data indicate the appearance of the maximal value of the cutoff in electroweak theory that cannot exceed the value of the order of 1 TeV. This prediction is made based on the numerical investigation of the lattice model on the finite lattices. However, as mentioned above, our main results do not depend on the lattice size.

ACKNOWLEDGMENTS

This work was partly supported by RFBR Grants No. 09-02-00338 and No. 08-02-00661, and by a grant for leading scientific schools 679.2008.2. The numerical simulations have been performed using the facilities of Moscow Joint Supercomputer Center.

-
- [1] Peter Arnold and Olivier Espinosa, *Phys. Rev. D* **47**, 3546 (1993); Z. Fodor and A. Hebecker, *Nucl. Phys.* **B432**, 127 (1994); W. Buchmuller, Z. Fodor, and A. Hebecker, *Nucl. Phys.* **B447**, 317 (1995).
 - [2] B. L. G. Bakker, A. I. Veselov, and M. A. Zubkov, *J. Phys. G* **36**, 075 008 (2009).
 - [3] M. A. Zubkov and A. I. Veselov, *J. High Energy Phys.* **12** (2008) 109.
 - [4] M. A. Zubkov, *Phys. Lett. B* **684**, 141 (2010).
 - [5] K. Holland, *Nucl. Phys. B, Proc. Suppl.* **140**, 155 (2005); Zoltan Fodor, Kieran Holland, Julius Kuti, Daniel Negradi, and Chris Schroeder, *Proc. Sci., LAT2007* (2007) 056 [arXiv:0710.3151].
 - [6] J. A. Casas, J. R. Espinosa, and I. Hidalgo, *Nucl. Phys.* **B777**, 226 (2007).
 - [7] According to the previous investigations of the $SU(2)$ gauge-Higgs model, this upper bound cannot exceed $10M_W$.
 - [8] F. Csikor, Z. Fodor, and J. Heitger, *Phys. Rev. Lett.* **82**, 21 (1999); *Phys. Rev. D* **58**, 094504 (1998); *Nucl. Phys. B, Proc. Suppl.* **63**, 569 (1998).
 - [9] F. Csikor, Z. Fodor, and J. Heitger, *Phys. Lett. B* **441**, 354 (1998).
 - [10] F. Csikor, Z. Fodor, J. Hein, A. Jaster, and I. Montvay, *Nucl. Phys.* **B474**, 421 (1996).
 - [11] Joachim Hein and Jochen Heitger, *Phys. Lett. B* **385**, 242 (1996).
 - [12] F. Csikor, Z. Fodor, J. Hein, J. Heitger, A. Jaster, and I. Montvay *Nucl. Phys. B, Proc. Suppl.* **53**, 612 (1997).
 - [13] Z. Fodor, J. Hein, K. Jansen, A. Jaster, and I. Montvay, *Nucl. Phys.* **B439**, 147 (1995).
 - [14] F. Csikor, Z. Fodor, J. Hein, and J. Heitger, *Phys. Lett. B* **357**, 156 (1995).
 - [15] F. Csikor, Z. Fodor, J. Hein, K. Jansen, A. Jaster, and I. Montvay, *Nucl. Phys. B, Proc. Suppl.* **42**, 569 (1995).
 - [16] F. Csikor, Z. Fodor, J. Hein, K. Jansen, A. Jaster, and I. Montvay, *Phys. Lett. B* **334**, 405 (1994).
 - [17] Y. Aoki, F. Csikor, Z. Fodor, and A. Ukawa, *Phys. Rev. D* **60**, 013001 (1999); *Nucl. Phys. B, Proc. Suppl.* **73**, 656 (1999).
 - [18] Y. Aoki, *Phys. Rev. D* **56**, 3860 (1997).
 - [19] W. Langguth, I. Montvay, and P. Weisz, *Nucl. Phys.* **B277**, 11 (1986).

- [20] W. Langguth and I. Montvay, *Z. Phys. C* **36**, 725 (1987).
- [21] Anna Hasenfratz and Thomas Neuhaus, *Nucl. Phys.* **B297**, 205 (1988).
- [22] One of the examples of such models is the Ginzburg-Landau theory of superconductivity.
- [23] The meaning of the words “potential barrier” here is different from that of the one-dimensional quantum mechanics as here different minima of the potential form the three-dimensional sphere while in usual one-dimensional quantum mechanics with the similar potential there are two separated minima with the potential barrier between them. Nevertheless we feel it appropriate to use the chosen terminology as the value of the “potential barrier height,” which measures the difference between the potentials with and without spontaneous symmetry breaking.
- [24] Y. Nambu, *Nucl. Phys.* **B130**, 505 (1977); Ana Achucarro and Tanmay Vachaspati, *Phys. Rep.* **327**, 347 (2000); **327**, 347 (2000).
- [25] M. N. Chernodub, *JETP Lett.* **66**, 605 (1997).
- [26] It has been shown in [3] that at the infinite value of the scalar self-coupling $\lambda = \infty$ moving along the line of constant physics we reach the point on the phase diagram where the monopole worldlines begin to percolate. This point was found to coincide roughly with the position of the transition between the physical Higgs phase and the unphysical symmetric phase of the lattice model. This transition is a crossover and the ultraviolet cutoff achieves its maximal value around 1.4 TeV at the transition point.
- [27] I. Montvay, *Nucl. Phys.* **B269**, 170 (1986).
- [28] W. Langguth, I. Montvay, and P. Weisz, *Nucl. Phys.* **B277**, 11 (1986).
- [29] M. I. Polikarpov, U. J. Wiese, and M. A. Zubkov, *Phys. Lett. B* **309**, 133 (1993).
- [30] Nambu monopoles in practice correspond to $SU(2)$ variables as the monopole configurations extracted from the hypercharge $U(1)$ field disappear at realistic values of coupling constants.
- [31] The inverse seems to us incorrect: the influence of non-perturbative effects on α_R is not suppressed by any small factor. We indeed observe that in the FR, where non-perturbative effects are large, the renormalized α differs from its bare value by about 50%, while far from the FR the difference is within 10% (for the lattice size $12^3 \times 16$).